Chem Soc Rev

Tutorial Review on Structure - Dendrite Growth Relations in Metal Battery Anode Supports

Journal:	*Chemical Society Reviews*
Manuscript ID	CS-TRV-07-2020-000867.R1
Article Type:	Tutorial Review
Date Submitted by the Author:	20-Aug-2020
Complete List of Authors:	Liu, Wei; Sichuan University, Liu, Pengcheng; University of Texas at Austin, Materials Science Program and Texas Materials Institute (TMI) Mitlin, David; University of Texas at Austin

SCHOLARONE™
Manuscripts

Tutorial Review on Structure - Dendrite Growth Relations in Metal Battery Anode Supports

Wei Liu [a, b*], Pengcheng Liu [c], David Mitlin [c*]

a: Institute of New-Energy and Low-Carbon Technology (INELT), Sichuan University, Chengdu, Sichuan, China, 610065

b: Engineering Research Center of Alternative Energy Materials & Devices, Ministry of Education, Sichuan University, Chengdu, Sichuan, China, 610065

c: Materials Science and Engineering Program & Texas Materials Institute, The University of Texas at Austin, Austin, Texas 78712, United States

** weiliu@scu.edu.cn, *David.Mitlin@austin.utexas.edu*

Abstract

This tutorial review explains the emerging understanding of the surface and bulk chemistry - electrochemical performance relations in anode supports (*aka* secondary current collectors, substrates, templates, hosts) for lithium, sodium and potassium metal batteries (LMBs, SMBs or NMBs, and KMBs or PMBs). In relation to each section, the possible future research directions that may yield both new insight and improved cycling behavior are explored. Representative case studies from Li, Na and K metal anode literature are discussed. The tutorial starts with an overview of the solid electrolyte interphase (SEI), covering both the "classic" understanding of the SEI structure and the "modern" insights obtained by site-specific cryogenic stage TEM analysis. Next, the multiple roles of supports in promoting cycling stability are detailed. Without an optimized support architecture, the metal-electrolyte interface becomes geometrically unstable at a lower current density and cycle number. Taking into consideration the available literature on LMBs, SMBs and KMBs, it is concluded that effective architectures are geometrically complex and electrochemically lithiophilic, sodiophilic or potassiophilic, so as to promote conformal electrochemical wetting of the metal during plating/stripping. One way that philicity is achieved is through support oxygen surface chemistry, which yields a reversibly reactive metal-support interface. Examples of this include the well-known oxygen-carbon moieties in reduced graphene oxide (rGO), as well as classic ion battery reversible conversion reaction oxides such as SnO_2.

Unreactive surfaces lead to dewetted island growth of the metal, which is a precursor to dendrites, and possibly to non-uniform dissolution. *Surveying the literature on various Li, Na and K metal supports, it is concluded that the key bulk thermodynamic property that will predict electrochemical wetting behavior is the enthalpy of infinite solution ($\Delta_{sol}H^{\infty}$) of the metal (solute) into the support (solvent). Large and negative $\Delta_{sol}H^{\infty}$ promotes uniform metal wetting on the support surface, corresponding to relatively low plating overpotential. Positive $\Delta_{sol}H^{\infty}$ promotes dewetted islands and a relatively high overpotential.* This simple rule explains a broad range of studies on Li, Na and K metal - support interactions, including the previously reported correlation between mutual solubility and wetting.

Introduction

The choice of anodes for Li/Na/K secondary batteries is a result of numerous considerations including the target energy and power, cycle life, manufacturability, cost, safety, *etc.*, as detailed in a recent review.[1] In categories such as cycle life, manufacturability, cost and safety, established ion battery anodes such as graphite continue to dominate without a rival in sight. For automotive applications, however, increasing the battery's energy has become a critical target, leading to interest in metal anodes.[2] Employing metal anodes (Li, Na or K) can result in a 50% increase in the gravimetric energy versus a conventional ion-insertion anode. The specific capacities of Li, Na and K metal anodes are 3861 mAh g^{-1}, 1165 mAh g^{-1} and 678 mAh g^{-1}, all far surpassing the capacity of graphite with Li (372 mAh g^{-1}) or of hard carbons with K or Na (250 - 350 mAh g^{-1} at low voltage).[3-6] For example, Li metal – $LiNi_{0.8}Mn_{0.1}Co_{0.1}O_2$ (NMC811) cathode cells can achieve 500 Wh kg^{-1}, which if commercialized would be transformative for the automobile industry.[3] Although the original battery created by Whittingham et al. was based on a Li metal anode, commercial LIBs remain based on the far less energetic graphite. Likewise, while emerging sodium and potassium - based secondary batteries could be based on metal anodes, most full-cell architectures employ carbons instead. Achieving long-term stable and safe metal anode plating/stripping performance is the key missing puzzle piece. This means that metal dendrites must be eliminated for the wide range of operating conditions to be potentially encountered in service.

Metal dendrites are ubiquitous in liquid-to-solid phase transformations and have analogues in gas phase-to-solid reactions, namely growth of various nanowires, microwires, nanotubes, etc.

A non-planar advancement of a growing solid front, which is what a dendrite is, can be driven by ion concentration gradients (electrochemical), temperature gradients (solidification), localized catalytic surfaces (nanoparticles used for growing nanowires), localized stress effects (extrusion of microfilaments), or combination of these factors. During electrochemical charging/discharging of a metal battery, dendrite growth at the anode is the overwhelming unresolved problem. Metal dendrites can penetrate the separator and lead to electrical shorting of the cell, resulting in battery thermal runaway, fires and even explosions.[3-6] An excellent summary of the various strategies for addressing the dendrite issues in lithium metal batteries (LMBs) may be found in a recent review by Luo et al.[7] Broadly, the strategies may be subdivided into dendrite suppression, dendrite regulation, and dendrite elimination, the last category involving novel approaches such as the use of external mechanical and magnetic forces. Dendrite suppression may be achieved by employing a solid electrolyte with functional fillers and by multifunctional mechanically strong membranes. Dendrite regulation may be achieved by controlling the Li nucleation sites, the growth pathways and the growth directions. Another strategy to suppress dendrites is through novel liquid electrolytes and additives, as detailed authoritatively by Kang Xu.[8]

Well-known analytical models have been established for nucleation and growth of metal dendrites, including the space-charge model, the surface nucleation and diffusion model, and the self-enhancing intensified electric-field density model. These models are all able to predict relevant electrochemical conditions leading to dendrite formation and growth.[5, 9] However, none are able to fully capture the spectra of environments where dendrites have been reported, including at low charging rates. These continuum models generally treat dendrite growth as being driven by solution concentration polarization, leading to localized space charge effects at the metal - electrolyte interface. The role of a growing and heterogeneous solid electrolyte interphase (SEI) has not historically been considered, although modern continuum approaches are beginning to make significant headway there. The older classic models would not be able to explain why in a wide range of liquid and solid electrolyte solvents, potassium and sodium metal anodes are much less stable than lithium anodes.[3, 5] The synergy between the metal and SEI instability appears to be extremely complex, having a dependence on a wide range of factors distinct from electrolyte ion transport polarization. For example, cross-over of cathode species have been determined to be an important factor in catalyzing unstable SEI, in-turn leading to

dendrites.[10] Dendrites have been reported to form and propagate at current density and plating capacity below space charge model predictions, and with concentrated salt solutions where ion concentration polarization is not expected.[3-6]

A key thrust of discussions in this article is the role of various supports with tuned interfacial chemistry and geometry/surface area in affecting dendrites. In parallel, stable vs. unstable SEI is considered to be a key aspect in determining whether the metal front becomes dendritic or remains planar. This is to some extent a different paradigm than what is reported in literature in terms of the dendrites destroying the SEI as they grow. There is strong emerging evidence of a reverse order: An unstable SEI destroys the planar metal front and leads to dendritic deposits, i.e., the unstable SEI occurring first rather than being a consequence.[11] A related discussion will be carried through this review. One point that also needs to be explored, is the synergy between the support and the SEI structure. It is not intuitive that the metal-current collector interface directly influences the SEI at the metal-electrolyte interface. Yet, indirect evidence from many articles indicates that the SEI structure of the baseline specimens (normally a commercial planar Cu or Al foil collector) evolves differently during cycling than in the optimized supports, often growing at a much faster rate and with relatively more organic vs. inorganic phases. However, this metal support - SEI relation is poorly understood and remains a critical topic for further study.

The motivation for this tutorial review article is to focus on both the fundamental background and on the recent exciting developments in controlling dendrite growth through tuned supports. There are literally hundreds of articles that have been published on supports with various architectures. While some are highly effective for preventing dendrites, others work only incrementally or not at all. It may appear that great success versus some success versus no success is often a matter of luck or of perseverance. Are researchers just taking an Edisonian trial-and-error approach, employing everything and anything in the materials chemistry toolbox? In this article, it is argued that this is not the case. Rather, metal supports that are effective follow rational materials design principles. The tutorial seeks to outline these material design rules, in terms of what is known and what needs to be understood further. Follow these rules the interface becomes stable, ignore them and one may observe dendrites rapidly forming. Through select case studies, it is illustrated how the different material design principles play into successful

support architectures. Throughout the review, topics are suggested where more research is necessary and where understanding is incomplete.

Solid Electrolyte Interphase (SEI): Overview and Recent Developments

The solid electrolyte interphase (SEI) layer is a spontaneously formed electrolyte reduction product that is present on a negative electrode's surface. A classical description of the thermodynamics related to SEI formation was provided by Goodenough *et al.*[12] In summary, when the lowest unoccupied molecular orbital (LUMO) of the negative electrode lies below that of the electrolyte with which it is in direct contact, electrons available from an external circuit will induce its reduction to a more stable product. This reaction is spontaneous, i.e. thermodynamically favorable. However, the process is kinetically self-terminating. The formed SEI blocks the electrolyte from being continuously reduced on the negative electrode's surface. It is normally assumed that the metal anode itself does not react with the electrolyte, although with K there is some evidence of chemical reactions occurring at open circuit potential (OCP). In general, the SEI consists of insoluble and partially soluble reduction products of various organic and inorganic electrolyte components containing Li, Na or K ions. An ideal SEI layer is fully adherent, with its thickness determined by the electron-tunneling range. In reality, the SEI layer is not fully self-passivating and continues to grow during cycling (it allows further electrolyte reduction), the extent of growth depending on electrolyte and ion type.[13]

In 1979 the concept of SEI was proposed by Peled *et al.* [14] **Figure 1A** shows this original mosaic model of the SEI that was envisioned to be present on lithiated carbons or on Li metal. The products of the reduction of salt anions are typically inorganic compounds like LiF, LiCl and Li_2O, which precipitate on the electrode surface. The reduction of the solvent also occurs, with the formation of both insoluble SEI components like Li_2CO_3 and partially soluble semi-carbonates and polymers. Edstrom *et al.*[15] revealed that a porous organic layer covers most of the surface of the compact inorganic inner SEI, suggesting that the solvent molecules do not react at the anode/SEI interface. In addition, the existence of polycarbonates exclusively in the outer layer of SEI was discussed by Novak *et al.*[16] The weaker Lewis acidity of Na than of Li leads to intrinsically higher solubility of Na-based SEI components and higher Na-metal reactivity towards liquid electrolytes.[17] The same may be argued for the K metal in relation to Li,

explaining its much higher reported reactivity with all carbonate and ether solvents. SEI formation has been shown to initiate below 1.5–1.25 V vs. Li/Li^+, Na/Na^+ or K/K.

Stability of the SEI is one key factor which determines the safety, power capability, shelf life, and cycle life of the battery. A stable SEI is an accepted prerequisite for safe battery performance. It is recognized that the structure of the SEI plays a crucial role in determining the cyclability of metal anodes. In-principle the SEI has the properties of a solid-state electrolyte, being electrically resistive but ionically conductive. A desirable SEI layer is also self-passivating with a stable thickness of a few nanometers, possessing high mechanical toughness (combination of strength and ductility), minimal solubility in the electrolyte, and wide temperature, current and voltage stability. These attributes ensure that the SEI will passivate the anode from further reducing the electrolyte, while allowing sufficient solid-state ion diffusion necessary for rapid electrochemical reactions.

The SEI serves multiple roles, including limiting further side-reactions between the metal and the electrolyte, as well as promoting uniform metal deposition by regulating the solid-state ion flux to the collector. It is accepted that the characteristics of the SEI, be it gradual vs. rapid growth, uniform vs. heterogeneous structure, are important indicators of interfacial stability. What is not yet established is the order of events; is a heterogeneous and/or unstable SEI a symptom of dendrites, or is it an underlying root cause? The two aspects do not have to be self-exclusive and may rather be synergistic. A heterogeneous (mechanical properties, thickness, ion transport, etc.) SEI will result in geometrical perturbations of the plating metal interface in regions where growth is kinetically favored. This is the SEI-leading-to-dendrites scenario. An advancing dendrite will cause further localized SEI formation, now around its leading edge. This is the dendrites-leading-to-unstable SEI scenario, since growth will be ongoing. One can then visualize the two processes being self-amplifying, where local SEI effects drive dendrites, which drive more local SEI, etc. Heterogeneity/instability in the initial SEI structure lead to further heterogeneity/instability in the SEI structure during repeated plating and stripping. As an alternative scenario, fresh SEI growth around a dendrite tip may seal off the solid-state diffusion path or mechanically impede its further motion. Hence in some cases the behavior may be self-terminating rather self-amplifying. At this point, the dynamic structure and the growth of the SEI around dendrites is not well understood. It is not known how the SEI structure directly adjacent

to a dendrite differs from the SEI structure in the same specimen but on a planar portion of the interface. Are there unique aspects of the portion of the SEI that covers a dendrite in terms of its thickness, phases, transport, mechanical, etc.?

Classical studies on SEI employed "global" characterization methods such as X-ray photoelectron spectroscopy (XPS) and infrared spectroscopy (IR) to reveal that ethylene dicarbonate $(CH_2OCO_2Li)_2$ was a major component. Further studies shown that the SEI exhibited a bilayer structure with an organic upper layer and an inorganic-rich inner layer. In addition to the ROLi-type species, other Li compounds such as lithium oxalate, Li succinate, acetals, orthocarbonates, orthoesters *etc.* were also identified.[18] The majority of SEI studies have been performed on lithiated graphite, silicon, tin and other insertion anodes relevant to ion batteries. However, with metals, one may not expect the same overall SEI structure, and would definitely not expect the same SEI formation kinetics. Lithium, Na and K metals are substantially more reactive than ion anodes. It has even been demonstrated that K and Na react with organic electrolytes at open circuit, *i.e.* without an external source of electrons.[19, 20]

To the authors' knowledge there have not been modern analytical studies that directly compare SEI structure on ion anodes and on metal anodes under analogous electrochemical conditions. Since surface and bulk analytical techniques have evolved tremendously over the last decade, it would be an interesting point to revisit in some detail. There would be value even in repeating some classic SEI analysis studies on the late 70 and early 80's using site-specific techniques such as cryogenic-stage transmission electron microscopy (TEM) as well as with modern electrolyte formulations. Solid-state ion transport within the SEI may significantly influence dendrite formation behavior. If the structure of the SEI for metal anodes is different than that for ion anodes, then so should be the solid-state ionic diffusivity. Differences in diffusivity, especially for the various dense inorganic phases, remain to be explored. Directly comparing ion diffusivity through Li_2O vs. Na_2O vs. K_2O, *etc.* is also a worthwhile topic for analysis, providing further insight on why Na and K dendrites are so prevalent.

Transmission electron microscopy (TEM) can uniquely provide high resolution site-specific information regarding crystallography of the metal and the structure/chemistry of the SEI. However, almost all battery materials are inherently TEM beam sensitive and many require

destructive sample preparation to obtain electron transparency. Because of their low melting point and relatively light weight, Li, Na and K metals are much more electron beam sensitive than ion anodes such as graphite or silicon. All SEIs are inherently beam sensitive too, the polymer-based phases having the propensity to cross-link under the electron beam. This makes it challenging to perform artifact-free quantitative analysis of metal anode interface by TEM. Typically, the metal anode samples have to be Focused Ion Beam (FIB) milled to electron transparency and transferred to the TEM without being oxidized through air exposure. The FIB and electron beam damage problem is becoming addressed through the use of cryogenic methods, although there are still issues with unintended (and unknown) sample modification. The recent advent of cryogenic transmission electron microscopy (TEM) has tremendously facilitated the analysis on electrochemically deposited lithium (EDLi) and its accompanying SEI.[21-23] Liquid - nitrogen stage TEM significantly reduces beam heating effects, which is important for both metal and SEI analysis. However even with liquid nitrogen cooled stages, electron beam damage will occur with sufficient dose. Athermal electron damage effects such as knock-on, radiolysis, and electron beam sputtering will not be mitigated by cryocooling.[24] For example, the knock-on threshold for Li of ~210 kV, giving potential problems when operating 300 kV instruments. Liquid-nitrogen stage "gentle" FIB milling sample preparation also remains capable of imparting damage to the materials, including ion implantation and introduction of nanoporosity. These challenges should by no means discourage future metal anode studies that rely on cryo-FIB milling and cryo-TEM analysis. Rather, it's the opposite, where the excitement is not only in materials discovery but also in techniques development. Caution is urged, however.

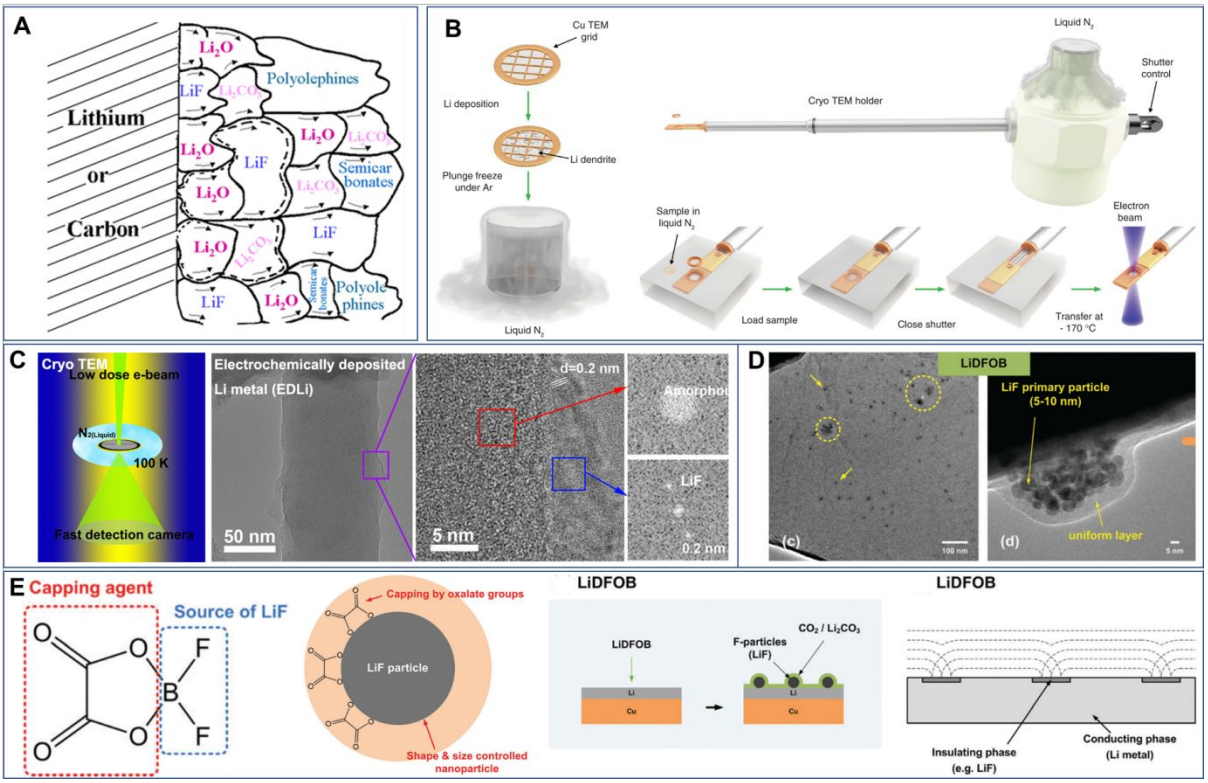

Figure 1. Illustrations of emerging techniques for SEI analysis. **(A)** Schematic of the classic Mosaic model for SEI structure.[18] **(B)** Schematic of liquid nitrogen cooled cryo-stage TEM sample preparation, transfer and analysis of Li metal dendrites.[21] **(C)** Cryo-TEM analysis revealing the amorphous plated Li metal and the SEI containing crystalline LiF.[22] **(D)** Cryo-TEM images of LiF particles in the SEI formed from LiDFOB in EC-EMC electrolyte. **(E)** (left) Proposed mechanism of LiDFOB acting as a capping agent for LiF nanoparticle generation, (center) model of SEI formed with LiDFOB, and (right) schematic of diffusion fields at lithium plated from each electrolyte.[25] *(A) Reproduced from ref. 18 with Open Access from IOP science, 2017. (B) Reproduced with permission from ref.21 American Association for the Advancement of Science (AAAS), 2107. (C) Reproduced from ref. 22 with permission from American Chemical Society, 2017. (D, E) Reproduced from ref. 25 with permission from The Royal Society of Chemistry, 2018.*

Cui *et al.* was the first to employ a cryo-transfer method without air exposure to directly move the Li metal samples from an electrochemical cell into the TEM [21]. **Figure 1B** provides a schematic of this procedure. Lithium metal was electrochemically deposited onto copper TEM grids, washed with electrolyte, and then immediately flash frozen with liquid nitrogen. At cryogenic temperatures, the electron-beam induced heating is minimized, allowing for artifact-reduced analysis of both Li metal and the SEI. The authors employed in spherical aberration–corrected TEM at 300 kV to obtain atomic-scale images of the structures, setting the stage for a wide range of site-specific atomic-scale analyses, not possible through other methods. Kourkoutis *et al.* employed cryo-STEM of a cryo-FIBed specimen to analytically map the phases

of a Li-based SEI in relation to each other and to the underlying metal.[23] Lithium hydride LiH was identified as a major inorganic constituent of the SEI that was adjacent to the Li. This an intriguing result, since per conventional surface science techniques LiH has not been widely reported as a SEI constituent.

Figure 1C illustrates another recent example of the cryo-TEM approach from work by Meng *et al* [22]. After a short plating time at intermediate current in a conventional electrolyte (5 min at 0.5 mA cm^{-2}, 1 M $LiPF_6$ in EC/EMC) the imaged Li metal was amorphous. The SEI layer over its surface was uneven. The SEI itself consisted of amorphous organic species and crystalline LiF. At longer deposition times, such as 2 hours, the Li metal became crystalline. Lucht *et al.* investigated the influence of electrolyte salts on the structure and morphology of Li-based SEI, these results being shown on **Fig. 1D**.[25] The authors employed cryo-transfer and cryo-stage TEM methods to image the key components of SEI structure. The electrolyte salts investigated include $LiPF_6$, $LiBF_4$, lithium bis(oxalato)borate (LiBOB), and lithium difluoro(oxalato)borate (LiDFOB), each dissolved in a mixture of ethylene carbonate (EC) and ethyl methyl carbonate (EMC). The LiDFOB electrolyte had significantly better cycling performance compared with $LiBF_4$ + LiBOB. Surface analysis by XPS indicated that the SEI was primarily lithium alkyl carbonate, Li_2CO_3, lithium oxalate, and LiF. The average composition of the SEI with $LiBF_4$ + LiBOB electrolyte was similar to that with LiDFOB. After 10 cycles in $LiBF_4$ + LiBOB the capacity faded, and the SEI composition became on-par with just LiBOB without the $LiBF_4$. TEM analysis revealed that the LiDFOB generated a dispersion of LiF nanoparticles covered by a smooth layer of Li_2CO_3 and lithium oxalate. The $LiBF_4$ + LiBOB salts resulted in less homogeneous SEI structure, with larger more coarsely distributed LiF particles and with less uniform coverage by Li_2CO_3 and lithium oxalate. Based on this analysis, the generation of nanostructured LiF particles is proposed to result from the presence of oxalate based capping agents within the same molecular component as the source of the LiF (LiDFOB). This is shown in **Fig. 1E**. It was argued that the presence of the nanostructured LiF particles results in a more uniform diffusion field, in turn leading to more uniform metal plating and stripping.

What these emerging TEM - based findings bring to the understanding of the SEI is the degree of its inherent heterogeneity and the role of phase distribution. Localized phase distribution within the SEI may be extremely important for dendrite suppression for a range of

Li, Na and K systems. This possible broad conclusion requires further analysis, for example for carbonate-based electrolytes, with Na and K metal, etc. Localized "hot spots" within the SEI where dendrites are favored to grow are likely to exist and need to be identified. To date, the vast majority of TEM studies have been performed on model support geometries (planar foils, wires, *etc.*) rather than architectures designed to enhance cycling lifetime. This is another frontier for research, combining support architecture studies with site-specific TEM. Could fundamental TEM-based studies of the SEI structure be extended to highly engineered support architectures? It is also recommended site-specific cryo-TEM analysis, especially of the SEI, is directly coupled with global surface science techniques such as X-ray Photoelectron Spectroscopy (XPS) and Time of Flight - Secondary Mass Ion Spectroscopy (TOF-SIMS). This will confirm the overall phase content, allowing for greater certainty in reporting new phases discovered by TEM.

Emerging Understanding of Supports

Anode supports (*aka* secondary current collectors, substrates, templates, hosts) for Li, Na and K metal are usually geometrically complex three-dimensional architectures with surface areas that are larger than that of standard Cu and Al collector foils. One straightforward effect of an increased support surface area is to reduce the overall electrical and ionic current density during plating/stripping. Classical continuum models focused on ion concentration in solution help to explain how that in-turn stabilizes the metal - electrolyte interface. Monroe and Newman considered the high-curvature tip of a dendrite and its role in promoting a local intensified electric field, causing it to become a preferential site for further deposition from solution, and hence becoming self-amplifying.[26] Chazalviel and co-workers published another widely recognized space-charge model to explain Li dendrite behavior.[27] It was shown that when ions are deposited from a dilute solution at a fast rate, their concentration near the plating surface decreases, giving a classic concentration - polarization profile at the interface. This results in a localized space-charge region, and preferential deposition at the pre-existing geometrical protrusions near which the solution ion concentration is higher. This effect is likewise self-amplifying, since as the dendrite extended outwards more solvated ions become available. Above the limiting current density J^*, ion depletion near the metal surface occurs at a characteristic Sand's time τ. The model predicts that dendrites appear at a time very close to Sand's time,

which represents the moment when the concentration of cations at the electrode interface drops to zero.[27]

$$\frac{dC}{dx} = -\frac{Jt_a}{FD}, \qquad (1)$$

$$J^* = \frac{2FC_0D}{t_aL}, \qquad (2)$$

$$\tau = \pi D\left(\frac{FC_0}{2Jt_a}\right)^2, \qquad (3)$$

where D, F, t_a, C_0, and J correspond to the ambipolar diffusion coefficient, Faraday's constant, the anionic transference number, the initial ionic concentration, and the applied current density, respectively. The metachronous depleting behavior of cations and anions at the electrode surface results in a local space charge (F^*C_c) and thus a high electric field (E) that leads to dendritic growth. The Sand's time formulation discloses how a reduced current density due to a higher substrate surface area is a factor in suppressing dendrite growth. With high surface area three-dimensional supports, enhanced stability is achieved through a reduction of effective current (J). Other ways to suppress dendrites is to increase the Li^+ transference number ($1 - t_a$) and bulk ion concentration through improved electrolytes.

Supports will also affect the nucleation/dissolution of the plating/stripping metal crystallites. Authors have explored the role of interfacial chemistry, bulk solubility, and stress interactions between the support and the plating metal in affecting the nucleation kinetics.[28-31] Such considerations would apply equally to planar and to complex support geometries. There are several steps involved in the electroplating process, including the ion diffusion through electrolyte, charge transfer, atomic surface adsorption, surface diffusion, crystallite nucleation, and crystallite growth. There are two distinctly quantifiable activation energies, which would be manifested as overpotentials (voltage more cathodic that 0 V) during electrochemical plating. During plating, there is an initial nucleation overpotential (η_n) spike, followed by a steady-state plateau overpotential (η_p). The nucleation overpotential is straightforwardly associated with nucleation of new metal nuclei either on a bare collector surface or onto a pre-existing metal anode surface. The former is the case for true-half cells and for "anode-free batteries", where the working electrode in its stripped state is a bare current collector. In many cases the working

electrode contains a metal reservoir, resulting in plating that occurs on nominally the same material. It's is expected and experimentally confirmed that the overpotential for nucleation on a bare collector surface differs from the overpotential for nucleation on a metal reservoir. The second plateau overpotential is associated with additional nucleation and growth of existing metal nuclei. This overpotential is more difficult to ascribe to one specific processes, since additional nucleation and growth of existing nuclei are expected to occur simultaneously. Strictly speaking, neither overpotentials can be zero. There will always be a kinetic energy barrier to nucleation of a new phase, be it for a solid-to-solid or a liquid-to-solid phase transformation. The subsequent plateau-related overpotential will be lower, presumably due to heterogenous nucleation on the pre-existing metal crystallites or on other defects. This overpotential may be small enough that it would be difficult to measure. This is especially relevant when the plating current density is set to ultra-low values allowing for diffusional relaxation of associated stress.

There have been a wide number of published metal anode support, hosts and template architectures that are successful in suppressing dendrites to a varying extent. The reader is encouraged to consider prior review articles where these architectures are systematically reviewed and categorized for LMB, SMB and KMB applications.[4, 5, 7, 9] Thermal infusion and electroplating are the two most widely adopted methods to incorporate Li, Na and K metals into them. Studies consistently point out that three-dimensional supports that are well-wetted by the plating metal are most effective. These structures will simultaneously reduce the effective current density and increase the number of metal nucleation/dissolution sites. There are also other general unifying features of effective supports. This includes three-dimensional macroporosity and mesoporosity, which the metal can readily penetrate during plating, and that will buffer the cycling-induced volume changes. There is also the need for high electrical conductivity but a neutrality towards SEI formation *per se*. The support structure has to readily conduct electrical current but can't be extremely catalytic towards electrolyte decomposition to form its own SEI. A well-tuned host architecture will also geometrically frustrate dendrite growth by its tortuous non-planar morphology, with successful examples being provided in refs.[32, 33]

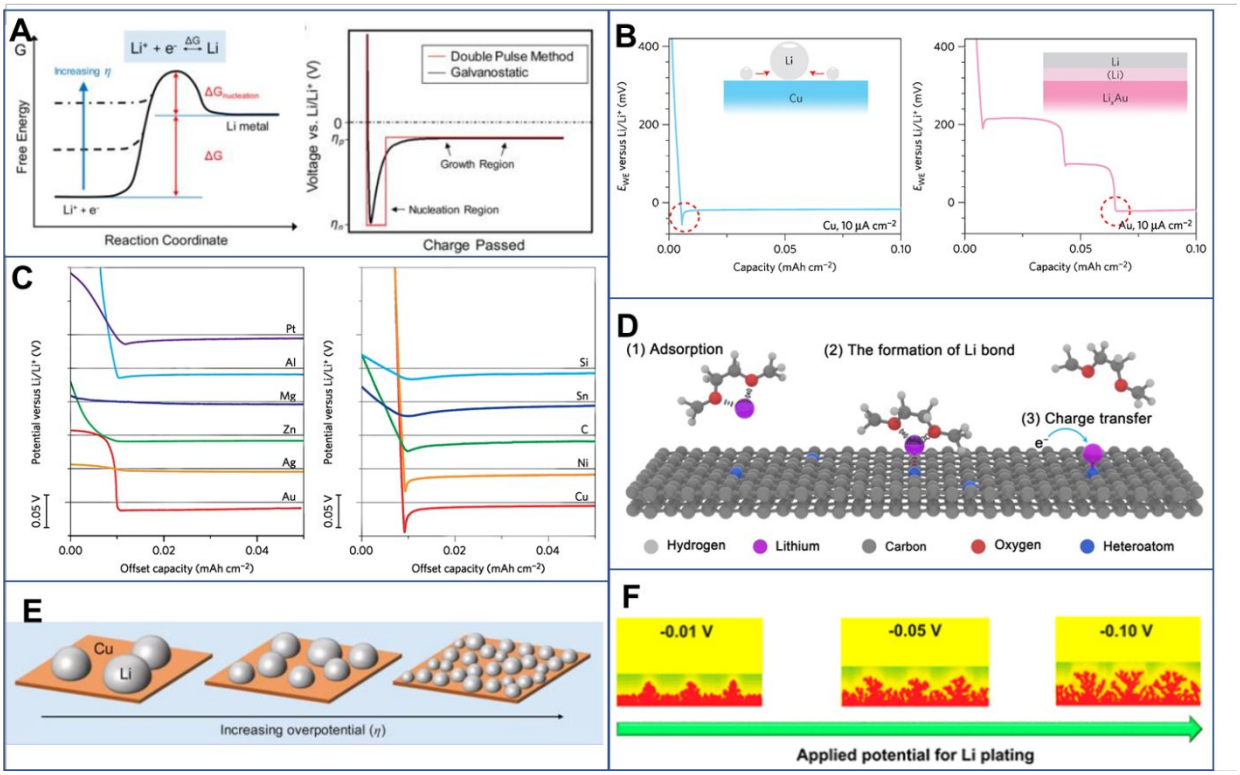

Figure 2. The role of metal - support energetics in film growth. **(A)** Schematic illustrating the relation between the energy barrier of Li metal nucleation and the plating overpotential.[28] **(B)** Comparison of the measured nucleation overpotentials of Li on Cu substrates versus on Au substrates. **(C)** Measured voltage profiles of Li plating onto various substrate with different solubilities for Li.[29] **(D)** Schematic illustration of solvated Li molecules on a carbon substrate containing heteroatoms.[30] **(E)** Schematic predicting the size and number density of Li nuclei is as a function of plating overpotential, based on simulation results.[28] **(F)** Simulated SEI fracture kinetics versus the applied overpotential, increasing overpotentials generating higher levels of interfacial stresses.[31] *(A, E) reproduced from ref. 28 with permissions from American Chemical Society, 2017. (B, C) Reproduced from ref. 29 with permissions from Nature Springer, 2016. (D) reproduced from ref. 30 with Open Access from American Association for the Advancement of Science(AAAS), 2019. (F) Reproduced from ref. 31 with permission from American Chemical Society, 2019.*

Figure 2A illustrates the these concepts,[28] relating the plating voltage overpotential to the Gibbs free energy ΔG through the Faraday constant: η = - ΔG/F. In literature, the initial plating overpotential has been correlated with lithiophilicity, sodiophilicity, potassiophilicity, *i.e.*, the affinity of the plating metal to wet the substrate. A "philic" support is one that in principle allows for facile nucleation of the plating metal, while a "phobic" support requires a higher driving force which translates into a more cathodic applied voltage. In literature, electrochemical philicty vs. phobicity has been correlated to thermal wetting of the molten metal onto the support in a dry

glove box environment. Light optically measured low wetting angles are meant to directly correlate with less cathodic overpotentials. This generally holds true during the first several plating cycles, with the two generally becoming more disconnected with increasing growth of the SEI. A thickening SEI would increase the ionic solid-state diffusional resistance, as well as resulting in stresses that oppose the volume changes associated with both the nucleation and the growth of the underlying metal film. In the authors' work, initially lithiophilic substrates have been observed to become increasingly lithiophobic (in terms of increasing overpotentials) with extended cycling.[11] This effect has been directly correlated with extensive SEI growth, per electrochemical and surface science analysis. It important to consider the cycling-induced evolution of philicity vs. phobicity since these may follow differing trends than the initial behavior. In principle, many of the design rules established over the last decade for optimized ion storage in carbons may be applied to metal plating supports. This also includes the ability to suppress extensive SEI growth, since the SEI catalyzing ability of the support itself is an important aspect in dendrite growth.[11]

It should be also pointed out that in many studies the reported overpotential is the average of the plating and the stripping values. Plating and stripping overpotentials would be symmetrical only for truly symmetrical cells, which possess identical support on both electrodes. The plating - stripping behavior in an asymmetric cell would follow an asynchronous kinetic path, for example if the working electrode was fully stripped at each cycle, while the counter electrode was a conventional thick metal foil. The measured overpotential is a combination of all resistances associated with that electrochemical step. In a two-electrode cell, one can't straightforwardly separate out the overpotential due to the plating working electrode versus due to the stripping counter electrode, or *vise-versa*. The best practice for obtaining accurate plating overpotential measurements is with a dedicated three-electrode cell, rather than with a standard two-electrode coin cell. If this is not possible, the counter electrode should possess stable and well-characterized electrochemical behavior, which is often challenging especially for K foils. Attention should be paid regarding whether a metal reservoir is employed on the working electrode or not, as the overpotentials will differ in each case. Plating on bare support - current collector is distinct from plating on pre-existing working metal. It should also be noted that overpotential measurements are normally carried out using a low current density, e.g. 0.01 mA cm^{-2}. This is done purposely to probe obtain quasi-equilibrium conditions. How these quasi-

equilibrium overpotentials affect intermediate and fast charge cycling behavior (where dendrites are most problematic) is not fully understood. In attempting to correlate dendrite growth to overpotentials, it would be useful to obtain their values at fast and intermediate charge rates, i.e. at rates where dendrites readily form. To date, there is insufficient understanding on how overpotentials at low currents extrapolate to fast charging.

Cui *et al.* found that the early stage plating overpotential is highly dependent on the bulk solubility of the support into the working metal.[29] As shown in **Fig. 2B**, electroplating Li onto Cu requires a substantial overpotential. Conversely electroplating Li onto Au requires a minimal overpotential, which was attributed to alloy formation at the interface, in-turn creating an intermediate buffer layer for facile nucleation. According to experimental galvanostatic curves shown in **Fig. 2C**, those metals which have considerable solubility with Li, including Pt, Au, Ag, Al, Mg, Zn, display low nucleation overpotentials. It is reasonable that the solubility of the metal in the support is an important criterion for lithiophilicity, and by extension for sodiophilicity and potassiophilicty. The intermediate buffering alloy layer conclusion is sound, with compositionally graded Si-Ge semiconductor layers serving as industrial example of an analogous approach for reducing nucleation stresses.

Another aspect that should be considered in parallel is whether solid-solution behavior is kinetically accessible, given the wide range of possible support surface structures. Gold is an example with nearly ideally accessible solubility. In various organic electrolytes, there is effectively nothing to block Li and Au interdiffusion. By contrast, highly stable passivating oxides such as TiO_2 or Cr_2O_3 are well-known as diffusion barriers. Their presence on a support surface would prevent chemical interactions between the metal and the support, making solubility kinetically inaccessible. Various surface oxide structures would possess different degrees of passivation, depending on the electrolyte and the reducing power of the working metal, *i.e.* Li vs. Na vs. K. Do stable ceramic oxide or nitride layers prevent interdiffusion of Li, Na and K with a support? How do these influence lithiophilicty, sodiophilicty, potasssiophilicty? Are there nanoscale oxidation reactions that occur at the interface that trigger or inhibit wetting behavior? How do secondary materials such as graphene or reduced graphene oxide, often placed on the surface of the collector, affect interdiffusion and alloying? If the metal - support alloying effect is primarily related to stress buffering, could carbon or polymer-based coating layers be

employed to achieve the same objective? Also, if Li_2O, Na_2O or K_2O are formed on the metal-support interface, what is their role during subsequent cycling? The structure of the metal-support interface would depend on factors such as the oxide's thermodynamic stability, the reducing strength of the contacting metal, as well as the applied voltage and current density. More experimental and modeling research is useful to understand such interfacial aspects.

Zhang *at al.*[30] performed simulations to explain why heteroatoms in a carbonaceous substrates that chemically react with Li will substantially lower the nucleation overpotential. This concept is illustrated in **Fig. 2D**. The modeling work went far in explaining the known lowering of overpotentials at early cycling due to oxygen-rich and nitrogen-rich carbon surfaces. The modeling also explained the experimentally observed poor wetting of the plating metal onto pristine CVD graphene supports, which possess minimal chemical interaction with the ions.[34]

One can make an argument that what matters for long-term dendrite growth are the overpotentials after extended cycling. Recent work on Li metal anodes compared lithiophilic reduced graphene oxide rGO membranes to lithiophobic "defect-free" graphene (df-G) membranes with low oxygen and structural defect content.[11] It was observed that as expected the rGO membrane initially yielded lower plating overpotentials. However, due to ongoing SEI growth during cycling the overpotential values with rGO rapidly increased. The cycling overpotentials with df-G were relatively stable, since SEI growth was not catalyzed by that carbon. By cycle 10, both the plating and the stripping overpotential with rGO was significantly higher than with df-G, making the initially measured lithiophilicity less relevant. Likely, with lithiophilic r-GO the Li metal plated on its surface. With lithiophobic df-G the Li metal plated beneath it, onto the current collector. Examining the role of support structure and chemistry in the long-term evolution of overpotentials is a promising area for more studies. How does the improved wetting due to metal - support reactivity balance against the potentially catalyzed SEI growth? How does the SEI with a poorly wetted support evolve as compared to the SEI with a well wetted support?

Lithiophilicity, sodiophilicity and potassiophilicity of carbons is dependent on their surface chemistry. For example, oxygen moieties, as well as adsorbed H_2O, O_2, CO_2, will react with metals to promote wetting. Pure CVD graphene, by contrast, does not react and leads to dewetted

islands.[34] One unexamined query concerns the cycling stability of carbon functionalities, since they reversibly react with the plating metal at every cycle. While O and N functionalities incorporated into the carbon lattice are likely at least partially retained, it is doubtful that the more loosely bound species are. At first plating, the surface adsorbed oxygen and water vapor likely becomes irreversibly incorporated into the oxide, hydroxide and the carbonate of the SEI. It is conceivable that after extended cycling, the carbon support surface becomes less reactive, leading to a gradual change in the wetting behavior. Carbon surfaces that initially led to conformal planar films, may ultimately promote island growth instead. More needs to be understood regarding whether and how these surface chemistries are retained during electrochemical cycling.

There is also an interrelation between the overpotentials and the SEI structure/stability. A high plating overpotential may accelerate SEI growth, while this growth will increase the overpotential further.[28, 31] Classical thermodynamics highlight the interdependence of the critical radius of the metal nuclei (r_{nuc}) and the electroplating overpotential (η_n): $r_{nuc} = 2\,\Gamma\,V_m/F|\eta_n|$, where Γ is the surface tension between deposited metal and electrolyte, V_m is the molar volume of Li, F is the Faraday's constant. One can directly deduce an inverse relationship between critical nuclei size and the overpotential. There is also a cubed correlation between nuclei number density and the overpotential. A larger overpotential, *i.e.* a larger driving force, results in finer crystallites being formed and in much higher numbers, as shown in the schematic in **Fig. 2E**.[28] In that study, the authors observed that the finer Li metal crystallites were associated with severe porosity in film that was filled by the SEI. The major implication of this now classic study is that as the overpotential increases during cycling, the film structure will naturally evolve to be more heterogenous, geometrically and chemically. Dendrite growth then may then be viewed as a predictable outcome of a microstructure that naturally evolves towards nonuniformity, as guided by nucleation thermodynamics. Hwang *et el.* performed dimensionless fitting of experimental transients of Li electroplating capacity.[31] The authors demonstrated that increasing overpotential also leads to increased stress in the SEI and to Li metal dendrite growth. Those results are shown in **Fig. 2F**. Mukherjee *et al* performed modeling work to demonstrate that dendrites can actually rupture the SEI layer.[35]

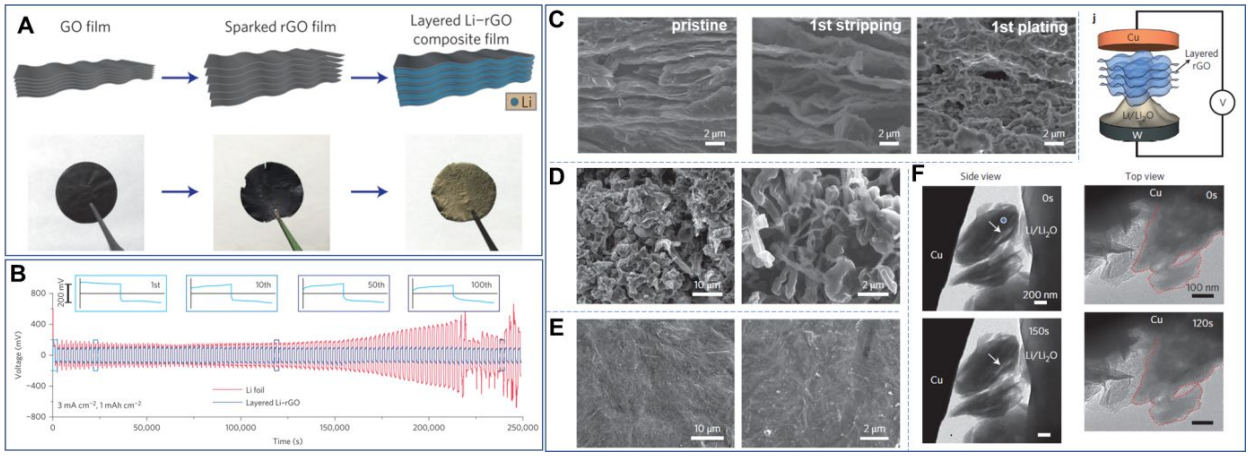

Figure 3. Example of an early embodiment for a lithiophilic Li metal support, based on flexible reduced graphene oxide rGO sponge. **(A)** Schematic for the fabrication process of a layered Li-rGO composite. **(B)** Galvanostatic cycling results for symmetric cell based on Li–rGO electrodes and Li foil baseline. Testing was performed at 3 mA cm^{-2} in 1M LTFSI in DOL-DME and 1 wt.% $LiNO_3$. **(C)** Cross-section SEM images of the Li–rGO electrode in as synthesized state, after first stripping, and after first plating. **(D)** and **(E)** SEM images of the bare Li foil surface and the Li–rGO surface after 10 galvanostatic cycles, respectively. **(F)** Time-lapse images showing the side view and the top view of an rGO film during the Li deposition process.[36] *Reproduced from ref. 30 with permission from Nature Springer, 2016.*

One of the earliest examples of templated nucleation was published by Cui *et al.*[36] The authors reported a composite partially reduced graphene oxide (rGO) - templated Li metal anode. The composite architecture exhibited low dimensional variation (~20%) during plating/stripping cycling and was flexible enough to withstand the associated volume changes. A schematic of the architecture and the Li-wetted composite electrode is shown in **Fig. 3A**. The composite containing 7 wt% rGO was fabricated through molten Li infusion into an expanded rGO support. The precursor for the support was graphene oxide (GO) that was placed into contact with the molten Li. A spark reaction occurred, expanding the film into a more porous structure. This phenomenon was explained by the sudden pressure release within the GO layers due to the removal of superheated residual water and surface functional groups, and the instant combustion of hydrogen formed during the reduction. This spark reaction generated the desired gaps for Li infiltration, while enough residual oxygen remained on the formed rGO to keep it lithiophilic. A flexible and well-wetted scaffold was obtained for subsequent electrochemical cycling.

An interesting aspect that should be noted about the architecture was that in regions where the GO film did not come in contact with the molten Li (e.g. the outer surface of the sponge in the

schematic), it remained unreduced and electrically insulating. This means that during cycling the outer surfaces of the sponge would not have Li plating on its surface. Because of this the Li would be protected from extensive contact with the electrolyte. This is an important point, since the architecture seems to have been able to achieve dual functionality as both a nucleating template and a protective membrane. Dual functionality architectures are extremely useful, since excessive SEI formation should be prevented if cycling stability is to be achieved. For the case of Na and K, which are markedly more reactive with electrolytes, dual functionality support/membranes should be even more useful. This Li - rGO sponge architecture also highlights the point that the most optimum oxygen-containing supports for promoting nucleation and wetting are partially reduced. In addition to being electrically insulating, stable oxides including GO will interact minimally with the plating metal. Likewise, inert carbon surfaces such as CVD graphene, are not wetted due to their lack of reactivity.[34] While it was reported that graphene capping layers are effective in maintaining a stable SEI,[37] these architectures serve as protective membranes and artificial SEI layers, with the metal plating beneath rather than on top.

In a carbonate electrolyte, the symmetric Li–rGO cells obtained stable cycling and stable overpotentials at relatively high currents, including at 3 mA cm^{-2}. These results are shown in **Fig. 3B**.[36] The Li–rGO anode retained up to ~3,390 mAh g^{-1} of capacity and exhibited ~80 mV overpotentials during cycling. By contrast, the baseline Li foils had unstable overpotentials. After 92 cycles the Li foil displayed a sudden voltage drop, followed by severe voltage fluctuations. **Figure 3C** shows the cross-section SEM images of pristine Li–rGO, after being plated and stripped, and after being plated, stripped and then plated again. When Li was stripped, the interlayer gaps originally occupied by metallic Li remained open. This illustrates that once formed, the expanded rGO structure remains expanded, with the remaining surface moieties probably being key for avoiding restacking of the graphene planes. After the Li was electrochemically plated back into the spacings, the electrode did display a different morphology as compared to the initially thermal impregnated composite. This indicates that the thermal Li impregnated microstructure is not fully representative of the electrochemically impregnated one. This aspect, the relationship between thermal wetting behavior and electrochemical wetting behavior, requires further exploration.

As shown in **Fig. 3E**, after 10 cycles, the layered Li–rGO surface remained smooth without observable dendrites. This was true even when the electrodes were tested at 3 mA cm^{-2} and 5 mA cm^{-2} current densities. After 100 cycles, SEI covered surface still exhibited a relatively smooth morphology. By contrast, the baseline Li foil exhibited mossy Li dendrites, as shown in **Fig. 3D**. To visualize the Li deposition behavior, *in-situ* transmission electron microscopy (TEM) was employed, using a specialized dual-probe biasing TEM holder, as shown in **Fig. 3F**. From the time-evolution edge-view images, it was observed that there was only a minor thickness change after Li deposition, indicating the stability of the rGO scaffold. When under the same conditions the Li was deposited onto a substrate without a host, dendrites were observed to rapidly form. The uniform Li plating/stripping was rationalized in terms of a large increase in the number of nucleation sites during plating, as well as interfacial protection. One question that is raised from these findings, and from numerous other studies on the role of supports in plating metal crystallite nucleation rates, concerns the optimum nucleation density. The above study demonstrates that excessive nucleation rate is deleterious due to concomitant roughness, porosity and SEI. Yet, it is also known that insufficient nucleation is deleterious due to increased local current density, formation of islands, etc. Combining experiments with simulation, it would be useful to probe this balance, attempting to find the sweet spot in nuclei density where the films are the most smooth, pore-free, conformal, etc.

A critical aspect for industry-wide adoption of lithium metal batteries is their ability to cycle at high current densities. Metal batteries must be safe at fast charge and discharge rates. According to space-charge model predictions, a higher charge (plating) current density causes more rapid ion depletion at the interface, giving rise to greater propensity towards dendrite growth.[27] During discharge (stripping), a higher current density may cause non-uniform dissolution of the metal, resulting in a geometrically rougher electrode surface, as well as "dead metal" (electrically isolated) in regions where dendrites dissolve at their base. Such scenarios have been experimentally verified.[5] For industrial applications, electrode areal capacity is in the 3 – 5 mAh cm^{-2} range. A relatively fast charge rate of 1C then corresponds to a current density of 3 – 5 mA cm^{-2}. More work is needed to understand dendrite growth in Li, Na and K metal at these higher current densities, where the classical Sand's time concentration polarization conditions would be applicable. Of course, for such fast charge behavior, dendrites will appear after fewer plating - stripping cycles. The dendrites may also undergo fundamentally different

growth phenomenology as compared to what is typically reported for extended cycling, e.g. 1 – 2 mA cm^{-2} for Li, and 0.5 – 1 mA cm^{-2} for Na and K. A key issue that researchers may have in reporting fast charge cycling behavior is that it will look significantly worse that the intermediate or slow charge cycling results. This may make it difficult to claim "state-of-the-art" cycling lifetime, often a pre-requisite for publishing in high profile journals. An increase in the community-wide recognition of the importance of high rate testing is therefore advocated.

Metal batteries also have to perform safely in wide temperature ranges, where ionic diffusivity in the electrolyte may be low (cold) or the SEI structure less stable (hot). To enable such rate and temperature capability while being free from dendrites, three main strategies are being pursued, often in parallel. One route is with improved electrolyte formulations.[8] The aim being to enhance the ion conductance in the electrolyte, by increasing the ion concentration and/or the diffusion coefficient of the solvated Li, Na or K ions. A complementary route, which is the focus of this tutorial, is to employ tuned supports to reduce the effective current density while promoting a “wetted” metal nucleation. A third route is to stabilize the SEI layer through various membranes, interlayers, and electrolyte additives. This approach has been the focus of several prior review articles.[2, 4, 7]

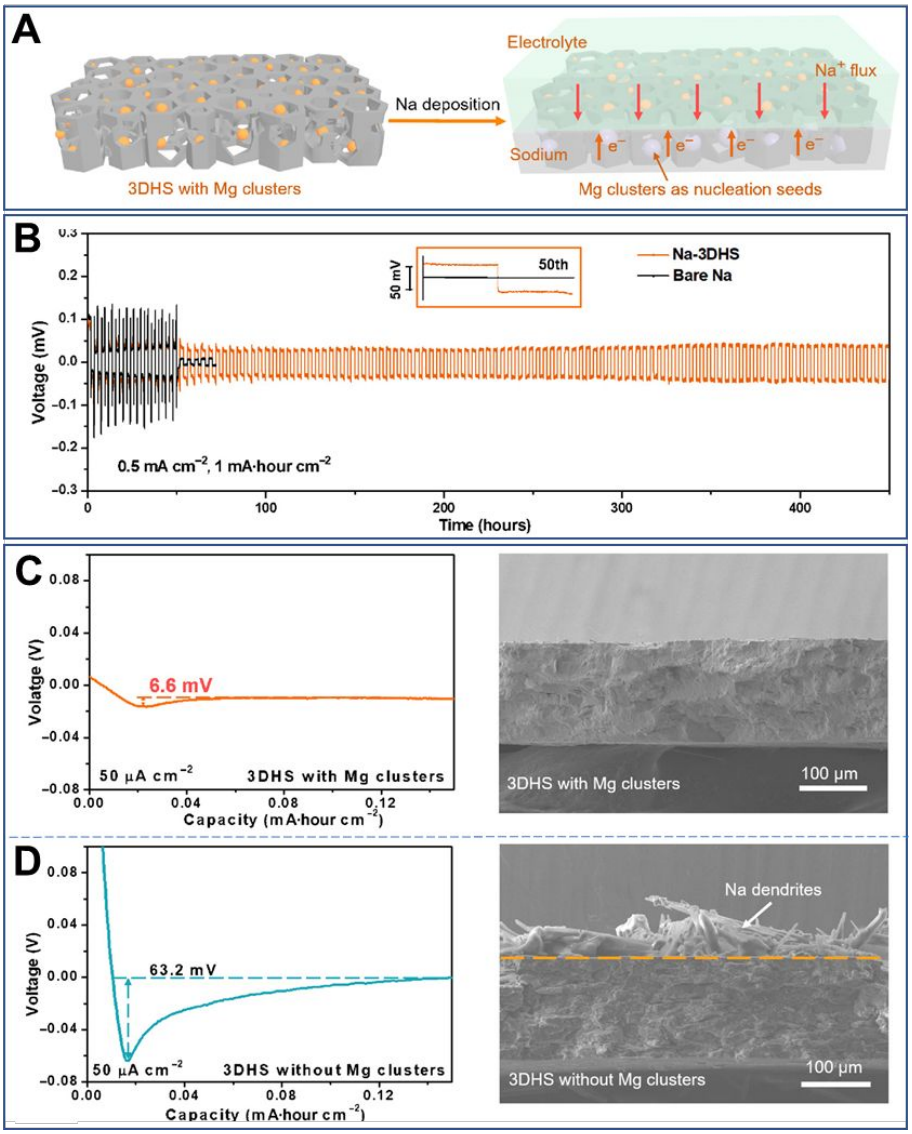

Figure 4. Example of a sodiophilic support, a three - dimensional hierarchical structure (3DHS) based on carbonized Mg-MOF-74 (Mg-based metal-organic framework–74) (cMOF74). (**A**) Schematic of Na deposition in the 3DHS film with Mg clusters. (**B**) Galvanostatic cycling results for symmetric cell based on Na-3DHS electrodes, also showing the Na foil baseline. Testing was performed at 0.5 mA cm^{-2} in 1 M $NaClO_4$ in EC-DEC with 5% FEC. Inset: Voltage profile at the 50th cycle. (**C**) and (**D**) Experimental overpotential curves (50 µA cm^{-2}) for Na deposition on the 3DHS film, with and without the Mg clusters. Also shown are the associated cross-sectional SEM images of the electrode after plating.[38] *Reproduced from ref. 38 with Open Access from American Association for the Advancement of Science (AAAS), 2019.*

Since Na and K metal anodes are more susceptible to dendrite growth than Li anodes, nucleation control becomes especially important. Yang et al. reported that Na metal can be controllably nucleated on surfaces of group II metals.[38] The rationale was based on solubility,

namely alloying of group II metals with Na, leading to reduced nucleation batteries. The authors reported that group II metal foils displayed much lower overpotentials (36.3, 35.5, and 12.1 mV for Be, Mg, and Ba, respectively) than those of Al and of Cu (53.0 and 44.9 mV). A novel Na plating support architecture that was based on Mg nanoclusters dispersed into carbonized MOF membrane with three-dimensional hierarchical structure was also employed, shown in **Fig. 4A**. The 3D hierarchical structure (3DHS) was based on a carbonized Mg-MOF-74 (Mg-based metal-organic framework–74) (cMOF74) containing Mg-based nanoclusters. An identical sample but with the Mg nanoclusters etched out was employed as a baseline. The electrode containing the Mg nanoclusters displayed promising cycling behavior, whereas the baseline did not. The Na metal was pre-plated into Mg - 3DHS using a current of 6 mAh cm^{-2}. During cycling the electrode was stable at 1350 hours when tested at 0.5 mA cm^{-2}, exhibiting low overpotentials in the range of 27 mV. This cycling behavior is illustrated in **Fig. 4B**. For the baselines, a short circuit occurred after about 50 hours. As shown in **Fig. 4C**, the Mg-nanocluster sample displayed an overpotential of 6.6 mV, when tested at 50 μA cm^{-2}. This is nearly an order of magnitude lower than for the baseline specimen, shown in **Fig. 4D**. SEM images of the two post-cycled surfaces, one fairly smooth while the other highly roughened, are presented in **Figs. 4C** and **4D**. Without the Mg nanoclusters, numerous sodium dendrites were observed.

This exciting study serves to illustrate the role of reversible (rather than fully stable) oxide-based templates in guiding nucleation. The Mg nanoclusters unlikely exist as pure metal, especially once submerged in an electrolyte containing some dissolved water and other sources of reactive oxygen. The standard enthalpy of formation for MgO is - 601.7 kJ/mol, whereas the standard enthalpy of formation for Na_2O is - 416 kJ/mol. The dramatic stability enhancement of the Na metal due to the nanoclusters may be a combination of solubility and reversible oxide effects. Since the nanoclusters are MgO on their surface, the oxide is likely an active participant in the wetting process. This may be through being reduced by the Na metal or through the formation of a ternary oxide phase(s). It is possible that there is a reduction of the MgO by the incoming Na. Since infusion was performed electrochemically, the applied voltage would drive this reaction akin to the well-known conversion chemistries that don't occur under thermal conditions e.g. $SnO_2 + 4Na^+ + 4e^- \Rightarrow 2Na_2O + Sn$, standard enthalpy of SnO_2 formation being - 580.7 kJ/mol.[39]

Xu *et al.* reported a 3D SnO_2-coated conductive porous carbon nanofiber (PCNF) framework (PCNF@SnO_2) as an effective host for K metal anodes [40]. The SnO_2 coating layer was essential for stable K plating, making the PCNF framework potassiphilic. The standard enthalpy of formation for K_2O is - 363 kJ/mol,[39] and a voltage driven $SnO_2 + 4K^+ + 4e^- \Rightarrow 2K_2O + Sn$ conversion reaction has been reported. In parallel, K does electrochemically alloy with Sn, giving credence to the alloying buffer layer for reduced nucleation barrier theory.[29] It is argued by W.L., P.L. and D.M. that lithiophilicity, sodiophiliocity and potassiophilicty are dynamic rather than static features of the plating and stripping process, with the reactive interface being an essential participant. For future studies, understanding the alloying and conversion reactions at the plating metal - support interface should be a research thrust.

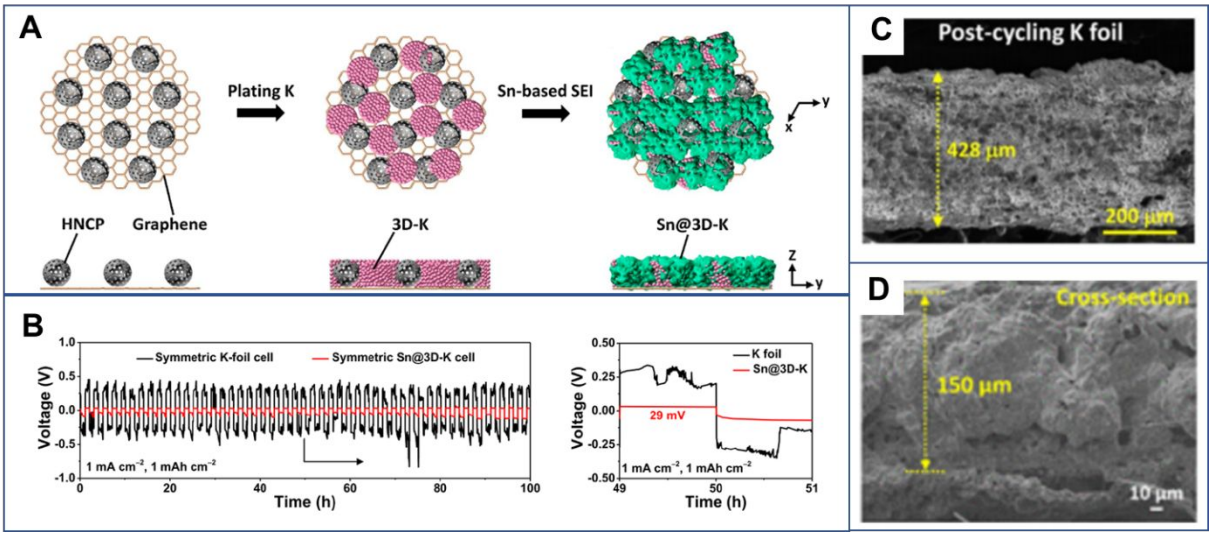

Figure 5. A three-dimensional potassiophilic host with a Sn-based SEI stability layer for K metal anode. **(a)** Schematic illustration for the hollow N-doped polyhedron/graphene is used as the conductive potassiophilic host, involving a graphene scaffold and Sn clusters. (**b**) Electrochemical performance, cycled at 1 mA/cm^2 in 0.5M KFSI in DME. **(c)** and **(d)** Cross section images of post-cycled pristine K metal and 3D-Sn hosted K metal, highlighting reduced volume expansion of the electrode due to 3D-Sn host.[41] *Reproduced from ref. 41 with Permission from American Chemical Society, 2019.*

A promising approach for achieving stable K plating and stripping, including in a full KMB with a ceramic cathode, was recently published by Sun *et al*.[41] This architecture termed Sn@3D-K is shown in **Fig. 5A**. Through a tailored three-dimensional architecture that included a surface layer for the metal, the authors simultaneously addressed the nucleation energetics and the SEI stability. A three-dimensional metal anode was synthesized by plating metallic K into hollow N-

doped C polyhedrons/graphene. This reduced the effective current density, provided an active surface for increased nucleation, and reduced the plating/stripping overpotentials. The SEI structure was controlled by employing a secondary reactive membrane between the potassium anode and the separator, which was based on K-active Sn. A direct chemical reaction between host K metal with Sn-TFSI solution was used to grow Sn-rich interfacial layer. The Sn layer was demonstrated to alloy and de-alloy with the K ions while the plating/stripping reactions were occurring. The K-Sn alloy would possess its own SEI, which was more stable than the native SEI formed on the K metal. The K metal was introduced into the conductive host by slow rate electrochemical deposition at 5 mhA cm^{-2}.

Stable plating-stripping cycling was achieved at currents as high as 1 mA cm^{-2}, which is impressive for K anodes. Dendrites were not detected, and a voltage hysteresis of ~31 mV was observed after 100 hrs. These findings are shown in **Fig. 5B**. By contrast, the bare K metal cell display fluctuating voltage profiles and much higher overpotentials. After cycling, the main SEI component of Sn@3D-K comprised of K_4Sn_{23}, SnO_2, K_2SO_3, K_2SO_4, KCl, KF, RO-K, and R-COOK. The post cycled baseline K showed SEI components of K_2CO_3, K_2HCO_3, KCl, KF, RO-K, and $R{-}OCO_2K$. After 100 plating-stripping cycles, the 3D-Sn hosted K underwent much less severe volume expansion (from 146 μm to 150 μm) as compared to bare K metal foil (from 367 μm to 428 μm), these results being shown in **Figs. 5C** and **5D**. This K metal structure was paired with $K_{1.56}Mn[Fe(CN)_6]_{1.08}$/graphene cathode in a full cell configuration, which was stable at 150 cycles at 1C.

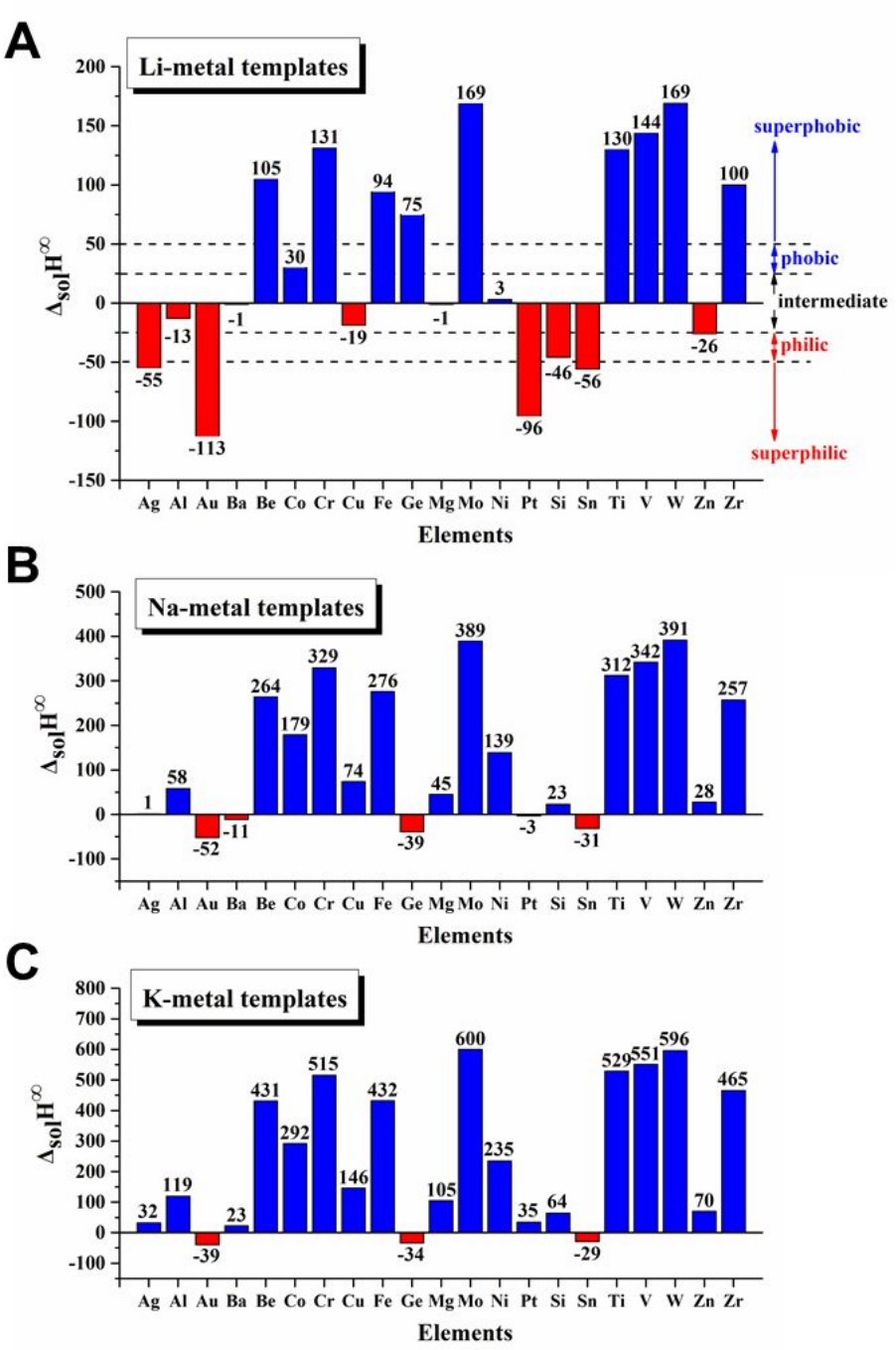

Figure 6. Tabulated enthalpy of mixing at infinite solution $\Delta_{sol}H^{\infty}$ (kJ/mol) for various elements with **(A)** Li, *i.e.* lithiophilicity, **(B)** Na, *i.e.* sodiophilicity and **(C)** K, *i.e.* potassiphilicity. [unpublished]. W.L., P.L. and D.M. propose that large negative $\Delta_{sol}H^{\infty}$ directly correlates with improved electrochemical wetting.

From the presented case studies, one can inquire about the general properties of a support that may be directly correlated to electrochemical lithiophilicity, sodiophilicity potassiphilicity? Is there thermodynamics-based criterion to predict electrochemical wetting of Li, Na and K onto

a support? It is concluded by W.L., P.L. and D.M. that a single bulk thermodynamic property is an accurate predictor: *At the onset of plating there is a limited amount of metal atoms diffusing into a much larger mole fraction of the support. The enthalpy of infinite solution ($\Delta_{sol}H^{\infty}$) of the metal into the support may be therefore used to predict the wetting behavior and the associated overpotential. The sign and magnitude of $\Delta_{sol}\,H^{\infty}$ is indicative of the thermodynamic affinity between the plating metal and the support, describing the driving force for their atomic mixing. Large negative $\Delta_{sol}H^{\infty}$ correlates with improved electrochemical wetting and correspondingly low plating overpotential. Positive $\Delta_{sol}H^{\infty}$ promotes dewetted islands with relatively higher overpotential.* One caveat is that the $\Delta_{sol}\,H^{\infty}$ value is likely most useful in predicting the early cycling wetting behavior, before there is significant SEI overgrowth on the support/metal surface. As discussed, an unstable SEI layer will drive up the plating and stripping overpotentials, thereby changing the wetting characteristics of the metal with cycle number.

Surveying the available literature, it appears that $\Delta_{sol}\,H^{\infty}$ correlates well with the experimental observations of philic *versus* phobic templates. **Figure 6** provides the room temperature $\Delta_{sol}\,H^{\infty}$ values for Li, Na and K with various supports, many of these having been experimentally measured, and others as potential research subjects.[44] Literature reported lithiophilic templates such as Au[29], Ag[45], Pt[46], Si[43], Sn[47], all have large negative $\Delta_{sol}\,H^{\infty}$, shown in **Fig. 6A.** The enthalpy criteria also explains the previously demonstrated sodiphilicity of Au[48], Sn[48] and Ba[38], as shown in **Fig 6B**. The ability of Sn to template K metals is also explained,[41] as shown **Fig 6C**. Oxides such as ZnO[42], CuO[49] and MgO[50] displayed good lithiophilicity with Li and SnO showed good sodiophilicity and potassiophilicity.[40, 41] The oxides that are effective are known as conversion anodes in Li, Na and K ion battery literature, such as the ones above. Could an $\Delta_{sol}\,H^{\infty}$ analogue be established for carbons containing various levels of structural and chemical defects? For carbon-based supports, it needs to be further understood to what extent does ion bulk solubility matter for wetting. Are best carbon-based supports for promoting lithiphilicty, sodiophilicty and potassiphilicity analogous in composition and structure to carbons that maximizes reversible ion storage capacity? For example, would there be major difference in the electrochemical wetting behavior of Li metal (highly soluble) vs. of Na metal (minimally soluble) on identical graphitic carbon based supports? This would be a confirmation of the enthalpy rule qualitatively applying to carbons as well (qualitative since there is a distribution of ion binding site energies). Systematic experiments would be useful for determining to what extent is the

Enthalpy of Mixing at Infinite Dilution criteria broadly applicable, and how well it can predict extended cycling behavior.

Future Prospects

In this section, several additional outstanding research questions and potential future research directions are presented. One general research thrust is to further investigate the structure of the Li, Na and K dendrites and the associated SEI. Specifically, it would be fruitful to understand the SEI structure and growth dynamics as a function of a broader range of electrochemical test parameters than has been analyzed to date. For example, what is the SEI structure for Li metal at the industrially relevant high current densities, such as 3 – 5 mA cm^{-2}? It is likely that the fast charging rate SEI structure will be quite different than the one obtained at for example 0.5 mA cm^{-2}. Moreover, how does the SEI vary with the total plated capacity, extended cycling, test temperature, static aging at OCP, *etc*.? The role of supports at this broad range of electrochemical conditions should be further examined too. It is conceivable that the low charging rate support-induced film wetting behavior and nucleation dynamics are modified by high current densities where solution ion concentration polarization – Sand's Time effects become manifested.

Another fruitful topic is further insight into aging process of the anode while being stored at various OCP, either charged or discharged. One can envision the SEI structure evolving during static storage, especially if the temperature is elevated. However, what about the actual film morphology? Can the metal anode surface roughness evolve during storage? Would surface energy consideration drive an initially conformal and smooth metal film to roughen over time, or to dewet becoming a series of disconnected islands? Unlike graphite, which is stable at room temperature, Li, Na and K metal anodes will rapidly self-diffuse and creep at ambient conditions. Over prolonged time, the evolution of the SEI structure and adsorption of impurities in the metal can lead to changes on the film wetting characteristics. For the three metal systems, the static stored at OCP aspect of metal film and SEI evolution has received only limited attention. Can dendrites grow through morphological changes in the metal, and without an external source of

electrons? Could stresses extrude the soft Li, Na and K through the "weak" regions of the SEI layer?

Details of the SEI structure may be obtained by a combination of post-mortem analysis of the cycled then disassembled cells, and in-situ / operando methods with dedicated transparent (light optical, conventional and high energy X-rays, neutrons, *etc.*) cell architectures. Globally averaged SEI structure and chemistry can be obtained by methods such as XPS, TOF-SIMS, while local SEI structure can be obtained by site-specific methods such as cryo-stage TEM, Tip enhanced Raman spectroscopy (TERS). Advanced analytical techniques would be useful in further quantifying the various roles that the tuned structure-chemistry supports may have in promoting stable cycling. Can enhanced electrochemical wetting be directly confirmed, allowing researchers to go beyond the current thermal wetting experiments? Site-specific cryo-stage TEM may be able to uniquely identify the SEI or support heterogeneities that lead to preferential metal dendrite growth at these sites.

Another scientific issue to be investigated is the role of localized Joule heating in dendrite and SEI formation, as well is the role of supports in dissipating the heat. SEI growth is associated with an increase in the interfacial resistance of the electrode, which manifests itself as an overpotential that increases with cycling. During cycling this polarization is dissipated as localized heat. For the low melting Li, Na and K metal and their SEI structures, there should be significant localized micro or even nanoscale thermal effects, that warrant further study. Both ion transfer and heat transfer across the SEI requires further modeling and experimental attention.

Lithium and especially Na and K are reactive towards a range of species, readily forming stable oxide, nitride, fluoride, and carbonate. The metals would react with entrapped water vapor, the generated HCl and HF, etc. In the solid-state electrolyte literature, the significant role of such impurities in electrochemical performance is becoming well-recognized. However, less is known for impurities in liquid electrolytes. This is especially the case for experiments performed using various tailored supports which are meant to react with the plating metal and may likewise react with the impurities. Reports on Li, Na and K dendrite morphology highlights a complex array of geometries despite comparable solvent - electrolyte formulations and electrochemical testing protocols. Could these differences be at least in part explained by study-to-study variation in

impurities? What is the role of chemical (rather than electrochemical) reactions of the Li, Na and K metals with its environment? How much of the isolated non-active "dead metal" is actually metallic, versus metal core - oxide shell or even fully oxidized? Is it possible to mechanically probe the metal vs. ceramic phases to identify their elastic and plastic properties, for example AFM or Nanoindentation? How do supports, many of which are rich in reactive oxygen, affect the metal surface chemistry and the SEI structure remains as an intriguing question as well.

Summary

With a standard untreated copper or aluminum foil current collector, the metal - electrolyte interface is more likely to become unstable and grow dendrites. This tutorial review discusses the structure - properties relations for metal anode supports, with an emphasis on potential future research directions. Effective metal anode supports go far beyond just reducing the effective current density during plating stripping, positively affecting the metal nucleation behavior, the film wetting characteristics, the geometry of growth and even potentially the SEI structure. Having an optimized support architecture is especially important for Na and K, since these metals tend to be highly reactive in conventional carbonate and ether electrolytes. Example case studies are presented for each of the three metal anodes, with key aspects of wetting and nucleation behavior being considered.

The tutorial begins with a discussion of the classic versus the modern understanding of the solid electrolyte interphase (SEI). An overview of how three-dimensional supports with tuned surfaces can improve the electrochemical performance is next provided. Multiple potential benefits are discussed, including the reduction of the effective current density, the increase in the metal nucleation rate during plating, improved film wetting behavior, the possibility of complex three-dimensional support geometry hindering dendrites, and the potential for SEI modification. It is concluded that an effective support surface chemistry is based on a reversibly reactive interface with the metal. This may be as oxygen - carbon moieties that may bind with the ions, or as conversion oxides such as SnO_2 that form Li_2O, Na_2O or K_2O and Sn. A thermodynamics-based criterion is established for metal wetting and associated overpotentials. It is proposed by W.L. P.L. and D.M that when the support shows a high negative enthalpy of infinite solution

($\Delta_{sol}H^{\infty}$) with the plating metal, improved wetting and reduced plating overpotential results. The highly effective Au-based, Mg-based and Sn-based support surfaces for Li, Na and K satisfy this rule. Support architectures that do not possess either a reversibly reactive surface chemistry or bulk solution behavior will impede electrochemical metal wetting, leading to island growth and increased overpotentials. During electrochemical cycling such islands will evolve into dendrites.

Acknowledgement

W.L. acknowledges financial support National Natural Science Foundation of China (51702223). D.M. and P.L. (conception of review, preparation of manuscript) were supported by the U.S. Department of Energy, Office of Basic Energy Sciences, Division of Materials Sciences and Engineering under Award # DE-SC0018074.

Key learning points:

1. Dendrites in lithium, sodium and potassium metal anodes are caused by a number of factors, including ion concentration polarization in the electrolyte, an unstable or irregular solid electrolyte interphase (SEI), and island-like nucleation and growth of the plating films.

2. The advent of cryogenic stage transmission electron microscopy (TEM) has allowed for site-specific quantitative analysis of the SEI structure. Among the new findings is that the distribution, not just the mean content, of the inorganic phases within the SEI greatly affects dendrite formation.

3. Supports (*aka* secondary current collectors, plating templates) with tuned surface area, geometry and interfacial energy can reduce concentration polarization by lowering the effective current density. Advanced supports will promote conformal growth/shrinkage of the films by reducing metal nucleation and growth energy barriers, *i.e.* the overpotentials. Supports may also affect the SEI structure, although this relationship needs to be further understood.

4. The effectiveness of supports in promoting electrochemical wetting of the plating metal translates into its planar versus island-like growth characteristics. The enthalpy of infinite

solution ($\Delta_{sol}H^{\infty}$) of the metal into the support may be used to predict wetting and the associated plating overpotential. A large negative $\Delta_{sol}H^{\infty}$ directly correlates with improved electrochemical wetting and a relatively lower overpotential, while a positive $\Delta_{sol}H^{\infty}$ leads to island growth.

References

1. J. Lu, Z. Chen, F. Pan, Y. Cui and K. Amine, *Electrochemical Energy Reviews*, 2018, **1**, 35-53.
2. H. Wang, Y. Liu, Y. Li and Y. Cui, *Electrochemical Energy Reviews*, 2019, **2**, 509-517.
3. J. G. Zhang, X. Wu and W. A. Henderson, *Springer*, 2017, **249**.
4. Y. Zhao, K. R. Adair and X. Sun, *Energy Environ. Sci.*, 2018, **11**, 2673-2695.
5. X.-B. Cheng, R. Zhang, C.-Z. Zhao and Q. Zhang, *Chem. Rev.*, 2017, **117**, 10403-10473.
6. J. Ding, H. Zhang, W. Fan, C. Zhong, W. Hu and D. Mitlin, *Adv. Mater.*, 2020, **32**, 1908007.
7. X. Zhang, A. Wang, X. Liu and J. Luo, *Acc. Chem. Res.*, 2019, **52**, 3223-3232.
8. K. Xu, *Chem. Rev.*, 2014, **114**, 11503-11618.
9. B. Lee, E. Paek, D. Mitlin and S. W. Lee, *Chem. Rev.*, 2019, **119**, 5416-5460.
10. H. Lee, H.-S. Lim, X. Ren, L. Yu, M. H. Engelhard, K. S. Han, J. Lee, H.-T. Kim, J. Xiao, J. Liu, W. Xu and J.-G. Zhang, *ACS Energy Lett.*, 2018.
11. W. Liu, Y. Xia, W. Wang, Y. Wang, J. Jin, Y. Chen, E. Paek and D. Mitlin, *Adv. Energy Mater.*, 2019, **9**, 1802918.
12. J. B. Goodenough and Y. Kim, *Chemistry of Materials*, 2010, **22**, 587-603.
13. A. M. Tripathi, W. Su and B. Hwang, *Chem. Soc. Rev.*, 2018, **47**, 736-851.
14. E. Peled, *J. Electrochem. Soc.*, 1979, **126**, 2047.
15. K. Edström, M. Herstedt and D. P. Abraham, *J. Power Sources*, 2006, **153**, 380-384.
16. P. Verma, P. Maire and P. Novák, *Electrochim. Acta*, 2010, **55**, 6332-6341.
17. R. Mogensen, D. Brandell and R. Younesi, *ACS Energy Lett.*, 2016, **1**, 1173-1178.
18. E. Peled and S. Menkin, *J. Electrochem. Soc.*, 2017, **164**, A1703-A1719.
19. T. Hosaka, S. Muratsubaki, K. Kubota, H. Onuma and S. Komaba, *J. Phys. Chem. Lett.*, 2019, **10**, 3296-3300.
20. D. I. Iermakova, R. Dugas, M. R. Palacín and A. Ponrouch, *J. Electrochem. Soc.*, 2015, **162**, A7060-A7066.
21. Y. Li, Y. Li, A. Pei, K. Yan, Y. Sun, C. L. Wu, L. M. Joubert, R. Chin, A. L. Koh, Y. Yu, J. Perrino, B. Butz, S. Chu and Y. Cui, *Science*, 2017, **358**, 506-510.
22. X. Wang, M. Zhang, J. Alvarado, S. Wang, M. Sina, B. Lu, J. Bouwer, W. Xu, J. Xiao, J. G. Zhang, J. Liu and Y. S. Meng, *Nano Lett*, 2017, **17**, 7606-7612.
23. M. J. Zachman, Z. Tu, S. Choudhury, L. A. Archer and L. F. Kourkoutis, *Nature*, 2018, **560**, 345-349.

24. D. B. Williams and C. B. Carter, in *Transmission Electron Microscopy: A Textbook for Materials Science*, eds. D. B. Williams and C. B. Carter, Springer US, Boston, MA, 2009, pp. 53-71.
25. S. Jurng, Z. L. Brown, J. Kim and B. L. Lucht, *Energy Environ. Sci.*, 2018, **11**, 2600-2608.
26. C. Monroe and J. Newman, *J. Electrochem. Soc.*, 2003, **150**, A1377.
27. J. Chazalviel, *Physical review. A, Atomic, molecular, and optical physics*, 1990, **42**, 7355-7367.
28. A. Pei, G. Zheng, F. Shi, Y. Li and Y. Cui, *Nano Lett.*, 2017, **17**, 1132-1139.
29. K. Yan, Z. Lu, H.-W. Lee, F. Xiong, P.-C. Hsu, Y. Li, J. Zhao, S. Chu and Y. Cui, *Nature Energy*, 2016, **1**, 16010.
30. X. Chen, X.-R. Chen, T.-Z. Hou, B.-Q. Li, X.-B. Cheng, R. Zhang and Q. Zhang, *Sci. Adv.*, 2019, **5**, eaau7728.
31. B. Thirumalraj, T. T. Hagos, C.-J. Huang, M. A. Teshager, J.-H. Cheng, W.-N. Su and B.-J. Hwang, *J. Am. Chem. Soc.*, 2019, **141**, 18612-18623.
32. K. R. Adair, M. Iqbal, C. Wang, Y. Zhao, M. N. Banis, R. Li, L. Zhang, R. Yang, S. Lu and X. Sun, *Nano Energy*, 2018, **54**, 375-382.
33. Y. Zhao, X. Yang, L.-Y. Kuo, P. Kaghazchi, Q. Sun, J. Liang, B. Wang, A. Lushington, R. Li, H. Zhang and X. Sun, *Small*, 2018, **14**, 1703717.
34. Q. Meng, B. Deng, H. Zhang, B. Wang, W. Zhang, Y. Wen, H. Ming, X. Zhu, Y. Guan, Y. Xiang, M. Li, G. Cao, Y. Yang, H. Peng, H. Zhang and Y. Huang, *Energy Storage Materials*, 2019, **16**, 419-425.
35. F. Hao, A. Verma and P. P. Mukherjee, *J. Mater. Chem. A*, 2018, **6**, 19664-19671.
36. D. Lin, Y. Liu, Z. Liang, H. W. Lee, J. Sun, H. Wang, K. Yan, J. Xie and Y. Cui, *Nat Nanotechnol*, 2016, **11**, 626-632.
37. K. Yan, H. W. Lee, T. Gao, G. Zheng, H. Yao, H. Wang, Z. Lu, Y. Zhou, Z. Liang, Z. Liu, S. Chu and Y. Cui, *Nano Lett*, 2014, **14**, 6016-6022.
38. M. Zhu, S. Li, B. Li, Y. Gong, Z. Du and S. Yang, *Sci Adv*, 2019, **5**, eaau6264.
39. G. V. Samsonov, *The Oxide Handbook*, IFI/Plenum, 1973.
40. X. Zhao, F. Chen, J. Liu, M. Cheng, H. Su, J. Liu and Y. Xu, *J. Mater. Chem. A*, 2020, **8**, 5671-5678.
41. M. Ye, J.-Y. Hwang and Y.-K. Sun, *ACS Nano*, 2019, **13**, 9306-9314.
42. H. Zhang, X. Liao, Y. Guan, Y. Xiang, M. Li, W. Zhang, X. Zhu, H. Ming, L. Lu, J. Qiu, Y. Huang, G. Cao, Y. Yang, L. Mai, Y. Zhao and H. Zhang, *Nat. Commun.*, 2018, **9**, 3729.
43. Z. Liang, D. C. Lin, J. Zhao, Z. D. Lu, Y. Y. Liu, C. Liu, Y. Y. Lu, H. T. Wang, K. Yan, X. Y. Tao and Y. Cui, *Proc. Natl. Acad. Sci. U. S. A.*, 2016, **113**, 2862-2867.
44. F. R. d. Boer, B. Boom, W. C. M. Mattens, A. R. Miedema and A. K. Niessen, *Cohesion in Metals*, Elsevier Science Publishers, Amsterdam, The Netherlands (1989), 1988.
45. C. Yang, Y. Yao, S. He, H. Xie, E. Hitz and L. Hu, *Adv. Mater.*, 2017, **29**, 1702714.

46. K. Wen, L. Liu, S. Chen and S. Zhang, *RSC Advances*, 2018, **8**, 13034-13039.
47. M. T. Wan, S. J. Kang, L. Wang, H. W. Lee, G. W. Zheng, Y. Cui and Y. M. Sun, *Nat. Commun.*, 2020, **11**, 10.
48. S. Tang, Y.-Y. Zhang, X.-G. Zhang, J.-T. Li, X.-Y. Wang, J.-W. Yan, D.-Y. Wu, M.-S. Zheng, Q.-F. Dong and B.-W. Mao, *Adv. Mater.*, 2019, **31**, 1807495.
49. C. Zhang, W. Lv, G. Zhou, Z. Huang, Y. Zhang, R. Lyu, H. Wu, Q. Yun, F. Kang and Q.-H. Yang, *Adv. Energy Mater.*, 2018, **8**, 1703404.
50. B. Liu, Y. Zhang, G. Pan, C. Ai, S. Deng, S. Liu, Q. Liu, X. Wang, X. Xia and J. Tu, *J. Mater. Chem. A*, 2019, **7**, 21794-21801.

Table of Contents Entry

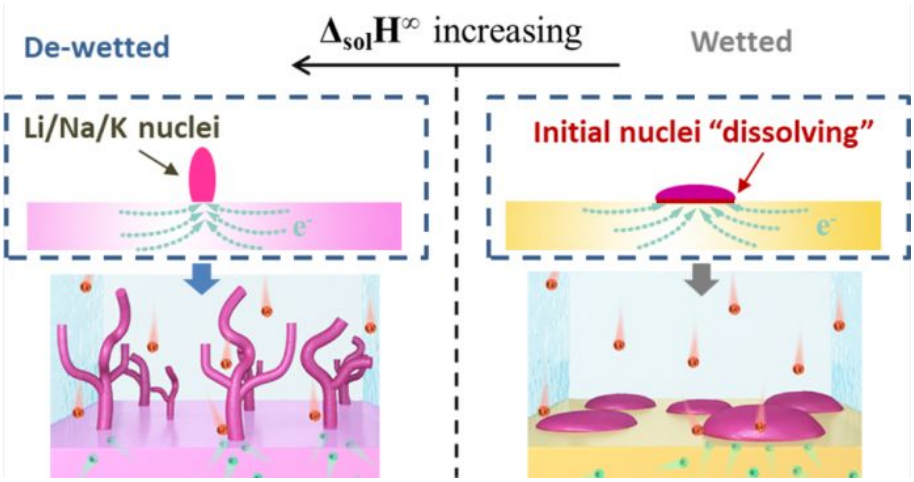

This tutorial review explains surface and bulk chemistry - electrochemical performance relations of lithium, sodium and potassium metal anodes.